Accepted for publication in Renewable Energy (Elsevier), 3 November 2023

# Theoretical approach to the scale effects of an OWC device

A. Molina–Salas[a], S. Longo[b], M. Clavero[a], A. Moñino[a]

[a]Andalusian Institute for Earth System Research, Universidad de Granada. Av. del Mediterráneo s/n. 18006, Granada (Spain)
[b]Dipartimento di Ingegneria e Architettura (DIA), Università di Parma. Parco Area delle Scienze 181/A, 43124 Parma (Italy)

**Abstract**

This research deals with the dynamic similarity problem for Oscillating Water Column (OWC) devices, for which air is the fluid that is subject to thermodynamic transformations in the inhalation/exhalation phases. Based on the differential problem, both linearised and full–nonlinear, the scale ratios satisfying similarity are calculated, with specific reference to the case where constraints are present on some of these scale ratios. The paper proceeds to identify the numerous processes of a turbulent interface that scales differently between model and prototype. With the aim of bringing to front the influence of the scale effects on featured aspects of the thermodynamic process involved, it is proposed that a non–equilibrium thermodynamics approach can be more comprehensive and representative not only of transformations, but also of scaling. The study reveals that in the case of OWC thermodynamics, non–equilibrium states which would be less evident in scaled model, would become more relevant as the scale is increased towards the size of the prototype, with consequences on performance.

*Keywords:* wave energy, oscillating water column, thermodynamics, scale effects, similarity, polytropic process

## 1. Introduction

The ocean dynamics appears as a potential source of renewable energy for primary conversion with an essentially permanent availability. Estimates suggests $\sim 10^7$ MW of off–shore available wave power over the coasts worldwide ([17], [7]), representing $\sim 34\%$ of the total primary conversion in Europe, [67]. In a world climate change scenario, it is a priority to develop technologies that allow to use the ocean resource for primary conversion as a complement/replacement of fossil fuels.

Nowadays, the Oscillating Water Column (hereinafter OWC) is the most remarkable wave energy converter device. One of its most important features is the fact that the only mobile element is the turbine, which simplifies the design and the costs of the device ([20, 54]). Several full–scale plants have been build: Mutriku (Spain), Pico (Portugal),

*Email address:* `amsalas@ugr.es` (A. Molina–Salas)

Port Kembla (Australia), and Niigata(Japan) among others. Nevertheless, different targets must be achieved to make this technology a real alternative, (i) to minimize the installation and deployment costs, (ii) to find technical solutions that make it an attractive framework for benchmarking, (iii) to find technical solutions to satisfy the end customers, or to get the social acceptance ([3, 27, 64, 49, 50, 51, 28]).

Different research lines have been focused on the development of the OWC devices. The theoretical performance of the OWC has been studied by solving analytically the radiation–diffraction problem ([10, 58, 11]); other research have focused on the power take-off (PTO) control and performance efficiency and management ([2, 16, 14, 21]). Some authors have studied the boundary conditions of the radiation-diffraction problem ([35, 39, 38]), as well as the implementation of the OWC embedded in vertical breakwaters ([45, 19]), the interaction between the OWC and the seabed and its long–time response ([55, 56, 41, 42]), the development of the floating OWCs to eliminate the problems associated with the installation in deep waters ([24, 57]), and the development of a new concept of turbine ([22]). Numerical simulations and experimental tests have been carried out to improve the knowledge about the OWC devices under controlled conditions, impossible to achieve otherwise, such as the hydrodynamic and aerodynamic coupling ([60]), the non–linear considerations to increase the OWC efficiency ([36]), and the implementation of the Actuator Disk Model for turbine simulations (see, e.g., [47]). The problem of physical and numerical modelling of the turbine is still open and discussed. In addition to the traditional Wells and impulse turbines, the construction and adoption of axial impulse turbines with design criteria already widely used in turbomachinery is proposed ([4]). In particular, wave-to-wire modelling has been conceived, with a holistic approach that includes turbine control ([5]). This means that the overall model includes three sections: (i) a primary converter model to convert wave motion into pressure fluctuations in the OWC; (ii) a secondary converter model to convert air pressure fluctuations into torque at the turbine axis; (iii) a tertiary converter model to convert torque at the turbine axis into electrical energy generated by an electric generator. The model is then used to optimize performance in relation to the plant location, as many parameters need to be tuned to maximize performances, including average annual wave statistics and inter-annual variability of the meteorological climate. All this in a context where the average price per unit of energy produced is still uncompetitive with many other energy sources, not least because of maintenance costs in an adverse environment; the overall yield is almost always in the single-digit percentage range. In order to resolve problems related to the social acceptance, some authors have studied the combination of OWC and hydrogen electrolysis for wave energy extraction and criteria management ([29]).

One key factor in the OWC performance is the thermodynamics of the air chamber. The efficiency of the device is closely related to the nature of the gas inside the chamber and its compression/expansion cycles, which results in a polytropic transformation. The application of the First Law of Thermodynamics to the open system of the air chamber can be done by *transforming* the open system into a close one ([31]). That process has been successfully studied under the assumption of the isentropic process of an ideal gas ([16, 59, 68]). Nevertheless, the implementation of the real gas model using the virial Kammerlingh–Onnes expansion helps to justify the low OWC efficiency values

([23, 53, 66, 63]). This fact is tested under experimental tests and numerical solutions of the radiation-diffraction problem with real gas implementation ([44, 43, 40]). Other researches point that the process is not totally adiabatic ([46]), as well as highlight the role played by the turbine as a restrain of the thermodynamic system, affecting the pneumatic efficiency ([46, 25]).

Although numerical simulations can provide information about the OWC performance, there are limitations when some specific features are implemented, such as the combination of dry air and moisture, the real gas model or the non–adiabatic process. Those problems can be solved using experimental tests which allow to reproduce situations in which different parameters can be controlled, impossible to control otherwise. The experimental tests must be done in a reduced scale to minimize the cost of the test and to adapt them to the space available in the laboratories. In this sense, the dimensional analysis allows to establish the scale between the real model and the prototype in order to ensure the prototype performance in the same way as the full–scale model. Nevertheless, in this scale transformation new problems can appear related to scale effects. These effects can be reduced or well quantified applying the dimensional analysis ([34]).

The scale effect affecting the OWC devices have been comprehensively studied by several authors, like [65, 8] among others. Traditionally, the scale factor has been calculated using the Froude similarity ([37, 13, 15]), with the particularity that the volume scale is $r_{\rho_w}\lambda^2$, where $\lambda$ is the length scale factor, and $r_{\rho_w}$ is the water density ratio ($\rho_{scaled\,model}/\rho_{prototype}$). Nevertheless, some authors have considered the problem separated into two parts: the hydrodynamic problem governed by the Froude similarity, and the aerodynamic problem governed by the Mach similarity. This solution leads to consider the same height of the chamber both in the model as in the prototype ([65]). Both peculiarities —the volume scale $V \sim \lambda^2$ and the constant height of the chamber— lead to the use of a rigid–walled bellow of air in the model ([12]).

The non–dimensional focusing on the OWC problem has been carried out under several scopes, namely hydrodynamic, aerodynamic and even thermodynamic ([65, 12, 48, 44, 46], among others). All in all, scale effects eventually present in the observations of model tests are difficult to identify and isolate from previous results, partly due to the fact that there is not enough information to compare. It would be desirable to have real data about thermodynamics variables to compare, but those variables have not been recorded in real–scale prototypes or they are not available, as far as the Authors in this research have been concerned.

The objective of this research is to develop a theoretical framework for a comprehensive understanding of the possible scale effects on the OWC performance and their interrelations, ultimately leading to a reliable estimate of the OWC efficiency. The dimensional analysis will focus on how the scale effects can affect to fundamental governing hydrodynamic and thermodynamic variables. In particular, the study points to the scale effect on the polytropic exponent, which determines the nature of the system process equation defining the air compression and expansion processes inside the OWC chamber.

This paper is organized as follows. First, the differential problem is introduced, describing the thermodynamic process in the chamber, providing similarity rules for the linearised problem –section § 3.1– and for the full-nonlinear problem –section § 3.2–. Section § 4.1 describes the similarity rules for the water side and section § 4.2 describes the scaling of the turbines, as alternative to hole and porous layer usually adopted for simulating quadratic and linear characteristics of the turbine. Section § 4.3 analyzes the scale effects due to non respecting Reynolds, Weber and Mach similarity, but only Froude similarity. Section § 5 describes an instability analysis for the polytropic exponent. Finally, discussion and conclusion sections bring to front possible links between governing variables affected by scale effect.

## 2. Reach and novelty of the research

This research focuses on the scale effects in the thermodynamic compression–expansion process from a primary theoretical approach, to be later implemented in experimental observation. As far as the Authors are concerned, no research is available in terms of scale problems of the whole OWC wave-to-wire setup. This research is intended brings to front a theoretical approach to the scaled OWC thermodynamics, as a reference to be later observed in experimental testing. All in all, there are prior experiences by other authors —Falcão & Henriques [12]— that reveal that the approach makes sense. This paper helps to understand how the thermodynamic scaling requires a different adjustment as the standard scaling applied to other process involved in OWC performance. In fact, the accuracy of thermodynamic processes experimentally simulated increases downward -from full scale to model-, due to the minimization of transient states between equilibrium states, while the rest of process involved in OWC performance gain in accuracy upward -from model to full scale. In addition, if a research focus in the wave–to–wire model, the accuracy that can be reached in other aspects, like the thermodynamics processes for example, will be lower, and vice versa. So it seems not totally feasible to get a great accuracy in all the different aspects of the whole process.

On the one hand, the study of the OWC chamber must be extended as a whole to the full problem. Otherwise, coupling different parts of the process that are in turn interrelated, might lead to a mismatched conclusions. However, in experience of the Authors in this research, a complete approach to the OWC system performance in which radiation-diffraction, turbine performance, power extraction and generator-to-grid connection would be otherwise a somewhat unreachable task. As far as the Authors are concerned, approaching the problem from different points allows to focus on specific aspects, yet to be clearly understood prior to build up a complete view. In that sense, state of the art reveals that this has been the way in which wave power extraction in general and OWC technology in particular have been studied. The theoretical formulation of the radiation-diffraction problem was conducted assuming pressure-air flow coupling based on a linearized isentropic relation —Evans [10], Sarmento & Falcão [58], Martins-Rivas & Mei [39, 38]—. Once the theoretical basis was settled, different research lines were devoted to advance separately on specific features of OWC performance, including turbine performance, turbine damping, chamber performance in which simplifications were assumed such as the replacement of the turbine by an orifice or an actuator disk model, wave action simulated by a piston type motion, etc.

Some authors —Henriques *et al.* [26], Ciappi *et al.* [5]— have successfully developed a complete wave-to-wire model that connects the wave action through the different transformations stages to the final connection to the grid. Even in the case, some simplifications have to be assumed when coming up with the pressure-air flow coupling, such as adiabatic process and replacement of the turbine by an actuator disk model, given the difficulties to represent the turbine performance. While that type of model provides with a really accurate approach to the complete process, there remain specific aspects that require a comprehensive yet detailed focusing. This is the case of thermodynamic properties bound to scale effects when dealing with experimental testing.

## 3. Dynamics and Thermodynamics of OWC

Let consider the system consisting of the air chamber in which the internal volume changes periodically as a result of wave action. Let us assume, for simplicity, that the air chamber is vertical cylindrical with a homogeneous cross-sectional area $A_c$. The turbine is schematised as having a pressure drop proportional to the velocity of the air flow exchanged with the external environment, or proportional to the square of the velocity, to schematise a Wells-type or impulsive-type turbine, respectively. The mass conservation equation reads:

$$\frac{\mathrm{d}m}{\mathrm{d}t} = -Q_m, \tag{1}$$

where $m(t)$ is the instantaneous mass of the gas (air) in the chamber and $Q_m$ is the mass flowrate exchanged with the ambient through the PTO cross-section. Since $m = \rho_c V$, where $\rho_c$ is the gas density in the chamber and $V$ is the volume of the chamber, eq.(1) can be written as

$$\rho_c \frac{\mathrm{d}V}{\mathrm{d}t} + V \frac{\mathrm{d}\rho_c}{\mathrm{d}t} = -Q_m. \tag{2}$$

The mass flowrate $Q_m$ can be expressed as

$$\begin{cases} Q_m = \rho_c A_{pto} v, & \text{during exhalation,} \\ \\ Q_m = \rho_a A_{pto} v, & \text{during inhalation,} \end{cases} \tag{3}$$

where $A_{pto}$ is the cross-section area of the PTO device and $v$ is the space average air velocity on $A_{pto}$, positive during exhalation and negative during inhalation. Here $\rho_a$ is the ambient air density. It is necessary to analyse the process of exhalation and that of inhalation separately, since in the former, air escapes from the chamber with a density greater than that at atmospheric pressure; in the latter, the density of the air flow is equal to that at atmospheric pressure.

The system evolution through equilibrium states addresses the polytropic process equation in its most general form

$$\frac{p_c}{\rho_c^n} = \text{constant}, \tag{4}$$

where $n$ is the polytropic exponent. We assume that the air behaves as an ideal gas, which implies that $n = \gamma$, where $\gamma = 1.4$ for air in adiabatic —or isentropic in the case of adiabatic and reversible— transformations, and $p_c$ is the absolute pressure in the chamber. The volume of the air in the chamber changes in time because part of it is periodically invaded by the water, hence

$$V = A_c \left(h_0 - \eta(t)\right), \tag{5}$$

where $h_0$ is the chamber height at rest and $\eta(t)$ is the instantaneous cross-section average water level in the chamber. As a first approach, we are neglecting the water column dynamics in the chamber, which results from the interaction between the OWC and the external wave field.

### *3.1. Similarity rules for a linear characteristic of the PTO device*

For a Wells turbine, as a first approximation we assume the following linear relation between pressure drop and air velocity:

$$p_c - p_a = K_1 v, \tag{6}$$

where $K_1$ with dimension $[K_1] = ML^{-2}T^{-1}$ is the air flow damping coefficient, assumed invariant during exhalation/inhalation, and $p_a$ is the absolute atmospheric pressure. In order to compare our analysis with previous analyses, we first express all the terms in eq.(2) as a function of the absolute pressure, obtaining the following differential problem:

$$\frac{\mathrm{d}p_c}{\mathrm{d}t} + \left[\underbrace{\frac{\gamma p_c}{A_c(h_0-\eta)}}_{\text{exhalation}}, \underbrace{\frac{\gamma p_c}{A_c(h_0-\eta)}\left(\frac{p_{0c}}{p_c}\right)^{1/\gamma}}_{\text{inhalation}}\right] \frac{A_{pto}(p_c - p_{0c})}{K_1} = \frac{\gamma p_c}{h_0-\eta}\frac{\mathrm{d}\eta}{\mathrm{d}t}, \quad \text{with} \quad p_c(0) = p_{0c}, \eta(0) = 0, \tag{7}$$

where $p_{0c}$ is the pressure in the chamber when $\eta = 0$, coincident with the atmospheric pressure. The system in eq.(7) represents a non-linear differential problem that can be numerically integrated upon defining the water level time function $\eta(t)$ inside the chamber. This problem is usually linearized in the hypothesis that $|\eta| \ll h_0$ and that the pressure chamber $|p_c - p_{0c}| \ll |p_{0c}|$, obtaining the following linear differential problem:

$$\frac{\mathrm{d}\tilde{p}_c}{\mathrm{d}t} + \frac{\gamma p_{0c}}{A_c h_0}\frac{A_{pto}}{K_1}\tilde{p}_c = \frac{\gamma p_{0c}}{h_0}\frac{\mathrm{d}\eta}{\mathrm{d}t}, \quad \text{with} \quad \tilde{p}_c(0) = 0, \eta(0) = 0, \tag{8}$$

where $\tilde{p}_c$ is the relative pressure in the chamber and $p_{0c} = p_a$.

If we indicate with the symbol $r_{(\ldots)}$ the ratio between the value of the variable $(\ldots)$ in the model and in the prototype, respectively, with the exception of the main length scale indicated with $\lambda$, imposing the dynamic similarity is equivalent to satisfying the following two equations:

$$\frac{r_{\tilde{p}_c}}{r_t} = \frac{r_\gamma r_{p_{0c}} r_{A_{pto}}}{r_{A_c} r_{h_0} r_{K_1}} r_{\tilde{p}_c} = \frac{r_\gamma r_{p_{0c}}}{r_{h_0}}\frac{r_\eta}{r_t}, \tag{9}$$

which refer the aerodynamic part of the OWC, to be added to the classical Froude similarity conditions for the hydrodynamic component. It is worth recalling that the invariance of the Froude number, in the model and in the prototype, requires that:

$$r_t = r_v = \lambda^{1/2}, \tag{10}$$

where $\lambda$ is less than unity for smaller than prototype models. Equation (10) implies the following scaling of some relevant variables: for the pressure it results $r_p = r_{\rho_w \lambda}$, where $\rho_w$ is the density of water and with $r_{\rho_w} \approx 1$ since water is also used in the model, although fresh water instead of salt water for OWC in the sea; for the flowrate it results $r_Q = \lambda^{5/2}$; for the acceleration it results $r_a = 1$. See [34] for the Froude scaling of other variables.

In similarity analysis, in theory, the number of unknowns exceeds the number of constraining equations, ensuring a sufficient number of degrees of freedom and, therefore, ease in selecting scales starting with the geometric scale, which is the most relevant constraint in physical modelling being, generally the length scale $\lambda < 1$ selected according to the laboratory facilities. In practice, other constraints arise for reasons of practicality and cost. Among these constraints, a particularly important one arises from the fact that the ambient pressure (outside the chamber) is the same in the model and in the prototype, forcing the condition $r_{p_{0c}} = 1$. In addition, by scaling the cross-section area of the chamber as $r_{A_c} = \lambda^2$, eqs.(9) reduce to

$$\frac{r_{\tilde{p}_c}}{\lambda^{1/2}} = \frac{r_\gamma r_{A_{pto}}}{r_{h_0} \lambda^2 r_{K_1}} r_{\tilde{p}_c} = \frac{r_\gamma}{r_{h_0}} \frac{r_\eta}{\lambda^{1/2}}, \tag{11}$$

or

$$\begin{cases} r_{h_0} = \dfrac{r_{A_{pto}}}{\lambda^{3/2} r_{K_1}} r_\gamma, \\[2ex] r_\eta = \dfrac{r_{A_{pto}}}{\lambda^{3/2} r_{K_1}} r_{\tilde{p}_c} = \dfrac{r_{h_0}}{r_\gamma} r_{\tilde{p}_c}. \end{cases} \tag{12}$$

Scaling $r_{A_{pto}} = \lambda^2$ and the PTO coefficient as $r_{K_1} = \lambda^{1/2}$, results in $r_{h_0} = r_\gamma \approx 1$ and $r_\eta = \lambda$. The condition of an invariant height of the chamber, in the model and in the prototype, as claimed by [65], is often replaced by the condition of $r_{h_0} = \lambda$ with the model chamber connected to an additional chamber with volume equal to $\Delta V_{c,m} = (\lambda^2 - \lambda^3) V_{c,p}$ (the subscripts '*p*' and '*m*' refer to '*prototype*' and '*model*', respectively). This similarity condition has been often adopted and succesfully tested, see, e.g., [37]. Note that, on the basis of eq.(9), the scale of relative pressures can be chosen at will, affecting only the scale of $\eta$ and $K_1$, but we do not forget that, in the present analysis, we are neglecting radiance effects (see [8]), assuming that the forcing $\eta(t)$ in the chamber is known a priori, a forcing that is instead calculated on the basis of wave motion outside the chamber considering scattering and radiation components of the potential flow describing the wave field.

An alternative approach is to adopt a different scaling for the coefficient $A_{pto}/K_1$. By imposing $r_{A_{pto}}/r_{K_1} \equiv r_{(A_{pto}/K_1)} = \lambda^{5/2}$, with a Froude scaling for the pressure, $r_{\tilde{p}_c} = \lambda$, results in

$$\begin{cases} r_{h_0} = \lambda r_\gamma, \\ r_\eta = \lambda^2, \end{cases} \tag{13}$$

which requires a chamber height in the model slightly smaller than $\lambda h_{0,p}$ since $r_\gamma \leq 1$, and avoids the need for the additional volume, as previously pointed out by other authors ([65, 12]). The vertical displacement of the water in the chamber of the model is reduced with respect to the classical $\lambda \eta_p$ value. Again, this approach is neglecting the interaction between the water dynamics in the chamber and the external wave field, and can be applied only for energetic sea state unless $\lambda$ is quite large; for instance, by assuming $\lambda = 1/10$ results $r_\eta = 1/100$ and a very small amplitude of the water oscillation in the chamber of the model equal to $\eta_{0,m} = 0.5\,\text{cm}$ for $H_p = 1\,\text{m}$, which does not make sense.

### 3.2. The analysis for the full non-linear problem

Up to this point, we have investigated similarity conditions with reference to a linearized model. We now consider the similarity for the full non-linear process expressed by

$$\frac{\mathrm{d}\tilde{p}_c}{\mathrm{d}t} + \left[ \underbrace{\frac{\gamma(\tilde{p}_c + p_{0c})}{A_c(h_0 - \eta)}}_{\text{exhalation}}, \underbrace{\frac{\gamma(\tilde{p}_c + p_{0c})}{A_c(h_0 - \eta)} \left( \frac{p_{0c}}{\tilde{p}_c + p_{0c}} \right)^{1/\gamma}}_{\text{inhalation}} \right] \frac{A_{pto}\tilde{p}_c}{K_1} = \frac{\gamma(\tilde{p}_c + p_{0c})}{h_0 - \eta} \frac{\mathrm{d}\eta}{\mathrm{d}t}, \quad \text{with} \quad \tilde{p}_c(0) = 0, \eta(0) = 0, \tag{14}$$

where a linear characteristic of the PTO is assumed.

For the exhalation process, we obtain the following similarity conditions:

$$\frac{r_{\tilde{p}_c}}{r_t} = \frac{r_\gamma r_{\tilde{p}_c}}{r_{A_c} r_{h_0}} \frac{r_{A_{pto}} r_{\tilde{p}_c}}{r_{K_1}} = \frac{r_\gamma r_{\tilde{p}_c}}{r_{h_0}} \frac{r_\eta}{r_t}, \quad \text{with} \quad r_{h_0} = r_\eta, r_{p_{0c}} = r_{\tilde{p}_c}, \tag{15}$$

which cannot be satisfied since the condition $r_{p_{0c}} = 1$ forces $r_{\tilde{p}_c} = \lambda = 1$, admitting only the trivial solution $\lambda = 1$.

For the inhalation process, the same conditions (15) hold, plus the additional constraint $r_\gamma = 1$ deriving from the additional contribution in the mass flowrate through the PTO. Again, an exact similarity cannot be obtained.

If we consider a polynomial characteristic of the PTO:

$$\frac{\mathrm{d}\tilde{p}_c}{\mathrm{d}t} + \left[ \underbrace{\frac{\gamma(\tilde{p}_c + p_{0c})}{A_c(h_0-\eta)}}_{\text{exhalation}}, \underbrace{\frac{\gamma(\tilde{p}_c + p_{0c})}{A_c(h_0-\eta)} \left(\frac{p_{0c}}{\tilde{p}_c + p_{0c}}\right)^{1/\gamma}}_{\text{inhalation}} \right] \frac{\tilde{p}_c}{|\tilde{p}_c|} \frac{A_{pto}\left(\sqrt{K_1^2 + 4K_2|\tilde{p}_c|} - K_1\right)}{2K_2} = \frac{\gamma(\tilde{p}_c + p_{0c})}{h_0 - \eta}\frac{\mathrm{d}\eta}{\mathrm{d}t}, \quad \text{with} \quad \tilde{p}_c(0) = 0, \eta(0) = 0, \quad (16)$$

the similarity conditions are:

$$\frac{r_{\tilde{p}_c}}{r_t} = \frac{r_\gamma r_{\tilde{p}_c}}{r_{A_c} r_{h_0}} \frac{r_{A_{pto}} r_{K_1}}{r_{K_1}} = \frac{r_\gamma r_{\tilde{p}_c}}{r_{h_0}} \frac{r_\eta}{r_t}, \quad \text{with} \quad r_{h_0} = r_\eta, r_{p_{0c}} = r_{\tilde{p}_c}, r_{K_1} = r_{K_2}^{1/2} r_{\tilde{p}_c}^{1/2}. \quad (17)$$

Again, only the trivial solution $\lambda = 1$ is possible if $r_{p_{0c}} = 1$.

In conclusion, the linearized process allows scaling to compensate for the constraint $r_{p_{0c}} = 1$ (i.e., the atmospheric pressure is the same, in the model and in the prototype); the full non-linear model does not allow this correction and necessarily brings scaling effects that are all the more relevant the more non-linearity is involved and the smaller the geometric scale.

It is convenient to highlight concepts related to the assumption that the process is adiabatic/isentropic. There is general agreement on the essentially adiabatic nature of the air expansion–compression process, considering the wave cycle period is small enough to prevent a complete heat exchange with the environment and boundaries —see Falcão & Justino [16] as example—. This hypothesis helps to simplify the pressure coupling through the continuity equation in the radiation–diffraction formulation and provides with a clear approach to the air compression–expansion analysis. However, deviations from strictly adiabatic conditions only, and further effects of moisture affecting the nature of the gas inside the chamber, lead to a more accurate view when focusing on possible causes for the low efficiency values observed in full scale prototypes. From the standpoint of First and Second Principles of Thermodynamics, which underlie the formulation of the energy–heat budget involved in compression–expansion, time as a variable is obviously missing in the definition of state functions representing equilibrium states. As far as the scale is concerned, it is clear that time scales involving both wave period and heat exchange in order to reach thermal equilibrium (prescribed by the Zero Principle of Thermodynamics) might lead to situations in which time required for heat exchange could be balanced with wave period depending on the scale factor, hence biasing the system performance from strictly adiabatic. A scale analysis reveals the extent to which those effects, in turn associated with time, can be negligible.

## 4. Other scale effects affecting the thermodynamics

Other issues related to the scale effects that affect OWC devices and related to the thermodynamics process of the OWC will be exposed below.

### 4.1. Similarity conditions for the water side

If the study of the OWC relates only to gas dynamics, the flow field of the water is assumed to be known within the chamber, and the water can be replaced, for example, by a piston with an assigned law of motion; equivalently, the dynamics of the liquid column in the chamber can be scaled almost arbitrarily. If, on the other hand (a rather frequent situation) it is the overall behaviour of the OWC that is of interest, including the interaction between air dynamics in the OWC and the wave field forcing the vertical oscillation of the water interface in the chamber, then the similarity of the water phase must also be considered. This similarity is Froude's similarity, naturally arising due to the fact that the restoring force of the water free surface is gravity, which faces the convective inertia of water.

We briefly recall that under the assumptions of water-wave theory, a potential can be used to describe the flow field, with $\mathbf{v} = \nabla\phi$, which satisfies the Laplace equation in the domain, $\nabla^2\phi = 0$, the condition of impermeability at the rigid walls, ($\partial\phi/\partial n = 0$ where $n$ is the normal at the wall) and the condition that the free surface is a trajectory where the Bernoulli theorem (neglecting the kinetic head) requires that

$$\eta - \left.\frac{1}{g}\frac{\partial\phi}{\partial t}\right|_{fs} = \begin{cases} \dfrac{\tilde{p}_c}{\rho_w g}, & \text{in the chamber,} \\ 0, & \text{out of the chamber.} \end{cases} \tag{18}$$

The next steps are based on Evans' method, which consists of decomposing the potential into the sum of a scattering component and a radiation component —see reference [10]—. Subsequent analysis would lead to calculating the two potentials, thus finding the solution to the problem that couples the dynamics of the air column in the chamber to the dynamics of water in the fluid domain. In practice, the wave field is distorted by the presence of the OWC. As a result of this, the fluctuation of the water column in the chamber is not known a priori, but is a non-linear function of the coupling between water column and air column.

Eq.(18) can be rearranged by decoupling the two variables $\eta$ and $\phi$, making use of the kinematic condition at the free surface:

$$\frac{\partial\eta}{\partial t} - \left.\frac{\partial\phi}{\partial z}\right|_{fs} = 0, \tag{19}$$

obtaining

$$\left.\frac{\partial\phi}{\partial z}\right|_{fs} - \left.\frac{1}{g}\frac{\partial^2\phi}{\partial t^2}\right|_{fs} = \begin{cases} \dfrac{1}{\rho_w g}\dfrac{\partial\tilde{p}_c}{\partial t}, & \text{in the chamber,} \\ 0, & \text{out of the chamber.} \end{cases} \tag{20}$$

The similarity conditions for the process described at the free surface by eq.(20) are

$$\begin{cases} \dfrac{r_\phi}{\lambda} = \dfrac{r_\phi}{r_t^2} = \dfrac{r_{\tilde{p}_c}}{r_{\rho_w} r_t}, & \text{in the chamber,} \\ \dfrac{r_\phi}{\lambda} = \dfrac{r_\phi}{r_t^2}, & \text{out of the chamber,} \end{cases} \tag{21}$$

where by definition of potential results $r_\phi = r_v \lambda$. The similarity conditions result in

$$r_t = \lambda^{1/2}, r_{\tilde{p}_c} = r_v \lambda^{1/2} r_{\rho_w}, \tag{22}$$

which permanently link the pressure scale in the chamber to the velocity scale in the water column.

### *4.2. Similarity for the turbine*

In the experimental approach for studying OWCs, it is common to replace the turbine with a hole or porous septum, which determine a quadratic ($\Delta p \propto v^2$) or linear ($\Delta p \propto v$) characteristic to simulate different types of turbines commonly in use. It is obvious that the characteristics of real-world turbines have a more complex functional structure, with torque, efficiency and resistance curves, which require bench measurements. A more complete analysis also requires the modelling of the generator, and is ultimately framed in a wave-to-wire model. In particular, the behaviour of the turbines also depends on the generator and the control system, in a model in which a large number of variables intervene that depend on both the turbine model adopted and the control system. Consider, in this respect, what is detailed in [26], in an analysis in which the numerous aspects that condition the overall efficiency of the system are analysed, including the behaviour of the turbines and the generator.

In a detailed analysis of the OWC, it is also imperative to adequately reproduce the turbine dynamics, which are characterized by sometimes very small scaling ratios. For example, aerodynamic forces and inertial forces, expressed as:

$$F_{aer} = \frac{1}{2} \rho_a C_r v^2 A^2, \quad F_{in} = \rho_a V \ddot{x}, \tag{23}$$

are scaled as

$$r_{F_{aer}} = r_v^2 \lambda^2, \quad r_{F_{in}} = \lambda^3 r_v r_t^{-1} \rightarrow r_{F_{aer}} = r_{F_{in}} = \lambda^3 \tag{24}$$

in Froude similarity and assuming that the $C_r$ has the same value in the model and in the prototype. With similar reasoning, the inertia of the rotor scales as $r_I = \lambda^5$, the mass of the blade scales as $r_m = \lambda^3$, the power scales as $r_P = \lambda^{7/2}$, the torque scales as $r_T = \lambda^4$.

However, in practical applications, it is difficult to construct the turbine in such a way that it respects scaling, since the mass of the propeller, for example, is usually too small and the inertia of the rotor is also difficult to scale correctly, unless $\lambda$ is not very small. In one of the few tests in literature carried out using a geometrically scaled impulse turbine with speed control through a servo-motor ([33]), the dimensions of the impulse turbine model could not be reduced to match the optimum damping ratio of the orifice. Turbine speed control is equivalent to an orifice with a variable diameter: as the rotation speed increases, the pressure drop also increases. In addition, the oversized turbine model also results in efficiencies that cannot be optimized in the OWC laboratory models, but which can be used to validate advanced numerical models of the chamber-turbine system and wave-to-wire models. Finally, the efficiency of the propeller blades is different in the model and in the prototype since the Reynolds number of the air is smaller in the model than in the prototype. To obviate, for example, the lower efficiency blade, it may be appropriate to change the shape of the profile, taking a tip from the vast literature originating from the development of drone blades, which are evidently characterised by low Reynolds operation.

An insurmountable scaling effect arises from friction, which is notoriously non-scalable and ends up playing a dominant role the smaller $\lambda$ is. This means that regardless of the construction materials adopted for the turbine, the adjustments that can be used to make airfoils that, at lower Reynolds numbers, have the same efficiency as the real airfoils, friction remains as a disturbing cause, reducing efficiency in the model much more than in the prototype. It is conceivable that a servo-driven turbine, with a controlled motor capable of reproducing the transient dynamics of real turbines to scale, could be a solution in cases where the complete simulation of the turbine becomes important for the model study of the OWC. See, e.g., [30] for an application of a hardware-in-the-loop approach to control wind turbines.

Attempting to implement all the information on the basic formulation might lead to conclusions that, in turn, can be hiding some relevant features. We have focused on the scale effect affecting the thermodynamic problem, as a feasible way to overcome the fact that, strictly speaking, time is not a variable included in the formulation of state variables, First and Second Principles and heat and energy budgets. Focusing on the scale effects, which in turn are inherently affected by scaled time, if not a complete way to implement time in the Thermodynamics formulation, it is feasible way to look into what relative differences might be expected when dealing with different scale prototypes.

On the other hand, it is important to highlight the difficulty of the construction of a scaled turbine connected to an electricity generator. Most of the experimental research have replaced the turbine with a porous septum or an orifice —see Thibeaut *et al.* [62], López *et al.* [37], Sheng *et al.* [59], Bingham *et al.* [1]— Even the Authors of the present research conducted numerical research using an actuator disk model —see Medina-Lopez *et al.* [40]—. Nevertheless, as a first approach, Authors of this research have performed some experimental test using a turbine, which implies to modify the relationship between pressure drop and air flow through it (linear in the case of the turbine, quadratic in the case of the porous septum). The next step would be to connect the turbine to an electric generation system, but this is not an easy task due to the friction induced to the turbine by the generator system, which can easily lead to an out–of–scale turbine model performance.

In addition, according to previous research by the authors —Molina *et al.* [46]—, the turbine acts like a restraint to the thermodynamic system. Therefore, its characteristics affect the thermodynamic compression–expansion process and, consequently, affect to the overall process. So, the replacement of the turbine with an orifice or porous septum would affect not only to the scale effects of the system, but to the overall performance of the device.

In conclusion, while a detailed analysis of the individual components is permissible as a first step, only an analysis of the entire OWC system allows the interdependencies between them to be studied. Suffice it to say that the damping of the OWC structure depends on both the geometry and the operating point of the turbine, which in turn is defined by a strategy to optimize the overall efficiency and power: every detail is important in order to determine with sufficient accuracy the efficiency of the entire system.

### *4.3. Scaling of turbulence and the effects of Reynolds, Weber and Mach numbers*

One aspect of scaling that is practically always overlooked is turbulence. The classical study of turbulence identifies a series of geometric and temporal scales, which are coupled by defining velocity scales. In this sense, the book by [61] is a clear example of a physical interpretation of turbulence on the basis of scales.

Turbulence in an OWC plays a major role and varies during the two exhalation–inhalation phases: in the first, turbulence is generated by the sloshing process and is strongly modulated in the compression phase, during which the vortices interact in a forced manner presumably different from the classical cascade scheme; in the second, atmospheric turbulence, near the turbine inlet, modulates the conveyed flow and invades the chamber after interaction with the blades. In both cases, at prototype scale, turbulence is seldom homogeneous and isotropic, and the spectrum deviates significantly from the classical Kolgomorov equilibrium spectrum. This also happens in the model, but it is intuitive that the scaling of variables is anything but straightforward and simple.

What is most interesting about the phenomena in the OWC, is the turbulent mixing that is coupled to the dynamics, defined as Level 2 in [9]. The most relevant aspect of that phenomena is the generation of baroclinic vorticity, due to the misalignment between pressure gradient and density gradient, i.e. between temperature gradient and entropy gradient. Vorticity of this nature facilitates the development of Kelvin-Helmoltz layers and consequent instability, with major effects on mixing. In this case, the coupling between mixing and flow field dynamics is due to the mixing's ability to reduce gradients, altering, in feedback, the generation of vorticity. If we want to evaluate these effects on scaling an OWC, it is intuitive that, for the same fluid (air, in the case of an OWC), the geometric size of the chamber is relevant in determining the level of heterogeneity, which is quite different for a full-scale OWC than for a reduced geometric scale model OWC. This means that some mixing mechanisms are not reproduced homothetically, leading to different process scales between prototype and model.

In practice, the structure of the turbulence is strongly influenced by the Reynolds number, which, in Froude similarity, scales according to $r_{Re} = \lambda^{3/2}$, being smaller in the model than in the prototype if $\lambda < 1$ and if $r_\nu = 1$, where $\nu$ is the kinematic viscosity. This applies to both the air and water side, the former being more important for the thermodynamic evolution of the system. Reducing the Reynolds number results in smaller time scales in the model than in the prototype if $r_{Re} = 1$. It also entails proportionally larger geometric scales: the separation of micro-vortices from macro-vortices is sharper if the Reynolds number is high. Since macro-vortices contain most of the energy, and micro-vortices contain most of the vorticity, if, in the transition from prototype to model, the ratio of density between the two classes of vortices varies, the distribution of energy and vorticity as a function of frequency (or rather, of the wave number) also varies accordingly.

The consequences of the scale effect on the distribution of energy and vorticity are quite relevant if we consider the transport processes (of heat, momentum, etc.) especially in the gas phase, which is the most thermodynamically active during cycles of an OWC. From this point of view, the diffusion of heat generated by the process of compressing the air in the chamber is commonly schematised by the Boussinesq model, assuming that it is proportional to temperature gradients through the thermal diffusivity, a phenomenological parameter similar to turbulent diffusivity. If the Reynolds number in the model is smaller than the Reynolds number in the prototype, the spatial gradients of the variables such as temperature, velocity, etc., will be smaller than they should be (this pattern is visually consistent with a more 'coarse' structure of turbulence at low Reynolds numbers) and thus the heat fluxes in the model will be smaller than they should be. We also remind that the Reynolds number can also be interpreted as the ratio of turbulent diffusivity to molecular diffusivity, $Re = uL/\nu \equiv \nu_T/\nu$ and thus smaller Reynolds in the model than in the prototype inevitably reduce the speed of momentum (and other variables) diffusion. It holds also for heat, entropy, and all the other quantities involved in the transformation.

During the inhaling process, the situation is even more complex. In the prototype, atmospheric turbulence is often quite intense, especially in the more energetic sea states usually accompanied by wind storms and bursts of turbulence. Depending on the measures taken to shield the turbine outlet, the flow entering in the chamber has a more or less high turbulence level, unlike in the model, which is normally tested in the absence of wind (unless a wind-wave tunnel is used) and therefore with zero or very small initial turbulence level. In addition, the turbulent flow of air at atmospheric pressure invades the chamber which, in the prototype, is full of air in depression characterised in any case by a non-negligible level of turbulence, while in the model it has a correspondingly lower level of turbulence than it should. The effect on turbulence due to the propeller blades is also present in the prototype, where the blades induce swirling (unless counter-rotating double propeller turbines are used) and, anyway, distorce turbulence, while the turbine is rarely installed in the model, due to the difficult scaling of certain variables such as rotor inertia and blade Reynolds number. To give an idea of the difficulties in stating similarity rules for similar cases, a summary of the complex scalings required for air turbulence and water turbulence during wind wave generation can be found in [6].

Another aspect to consider is the scaling of the Weber number, which is clearly not unitary if water is also used in the model since, in Froude similarity it results $r_{We} = \lambda^2$. A relatively low surface tension facilitates the incorporation of air into the water phase and the generation of droplets in the air phase. In the model, on the other hand, the size of the eddies and the turbulent velocity scale are too small for dominating the surface tension and therefore both foam and droplets are not or are rarely present. This has consequences, in the OWC chamber, mainly for the thermodynamics of the gas, since the gas lacks the characteristic spray and therefore has different thermodynamic properties than in the real world.

In addition, we remind that the Mach number also scales according to $r_{Ma} = \lambda^{1/2}$ in Froude similarity, being smaller in the model than in the prototype. This means that, in addition to the compressibility of air, which we have already discussed at length, the pressure waves that inevitably characterise water and air in the chamber also have a more damped effect in the model than in the prototype. The shock phenomena that might occur in the sloshing of air-water mixture in the chamber of the real OWC device (with consequent dissipation of energy) ([52]) certainly do not occur in the model, introducing an additional scaling effect.

All in all, while it is difficult to quantify the scale effects on turbulence and it is impracticable to eliminate them (it would require a gas, in the model, with kinematic viscosity reduced by a factor of $\lambda^{3/2}$ compared to air), it is immediately apparent that the thermodynamic transformations that occur, and which in physical reality are always non-equilibrium, are also more so in the prototype than in the model. As a consequence, classical thermodynamics based on quasi–equilibrium states works with a different approximation level for the model than for the prototype, and a non–equilibrium thermodynamics approach is more suitable (see, e.g., [32]). Non-equilibrium thermodynamics demands to be implemented for a number of good reasons, i) it provides an accurate description of the coupled transport processes; in the case of OWC we have already classified the quantities transported, i.e. mass, heat, moisture; ii) it quantifies the production of entropy, lost work and lost exergy; iii) it provides the entropy budget to be used in thermodynamic modelling. These conclusions should be taken into account when extrapolating laboratory data to the real data.

The foregoing discussion reveals the influence of the scale factor in the dimensional variables governing the problem. However, for thermodynamic system parameters the eventual influence of scale, i. e. the reference volume size of the gas system enclosed in the chamber, might not be so evident. The scale effect can modify the thermodynamic response through parameters that are not explicitly dependent on the system volume, hence on the representative length scale. That is the case of the polytropic exponent defining the system process equation —see equation (4)—. While a first approach might lead to assume $r_\gamma = 1$ following the non dimensional nature of the polytropic, it will be shown later in § 5.1 that a dependence on the length scale can be formulated through non–equilibrium instability approach.

In conclusion, all these scale effects, which cannot be eliminated for reasons of cost or because there are no fluids matching with the scale requirements, such as density, viscosity, surface tension or compressibility, must nevertheless make extrapolations of model measurements to the real thing extremely cautious, and push towards the realization of models at scales that are not excessively small. The classic suggestion to make at least two models with different geometric scales, so as to estimate the trend of the scale effects in order to extrapolate the correct results to reality, is still valid and appropriate, even if it comes up against a doubling of the experimental workload and costs.

## 5. Instability analysis

The air expansion–compression process in the OWC device follows a polytropic process characterized by the polytropic exponent $n$ as indicated in equation (4). In this case, if the thermodynamics is to be affected by any scale effects to be considered in the experimental tests, those effects might be represented through the polytropic exponent $n$ and its intrinsic dependence on system variables, that in turn can be affected by the scale of the problem, e. g. the system volume.

Indeed, Thermodynamics essentially deals with equilibrium states, with state functions not defined for transient ones. However, many process could never reach an equilibrium state in a strict sense, neither because the nature of the process itself, nor because the size of the system. For example, let us consider a process where there is a cyclical heat exchange. Therefore it is reasonable to think that the smaller the system the faster the thermal equilibrium can be reached. In the case of the air expansion–compression process of the OWC device, some scale effects could appear during scale model tests. Hence, an instability analysis applied to the polytropic exponent around an equilibrium volume $V_0$, can reveal some information on such effects.

The most general expression of the polytropic exponent is:

$$n = \frac{m}{K_T p} \tag{25}$$

where $m$ is the polytropic index —which is a relation between the specific heat under constant pressure, volume and a certain variable $y$—, $K_T$ is the isothermal compressibility coefficient, and $p$ is the pressure. The specific heat under any variable $x$ is defines as $C_x = T\left(\partial S/\partial T\right)_x$, being $S$ the entropy and $T$ the temperature. So, the polytropic index depends on these two variables, $m = f(S, T)$. On other hand, the isothermal compressibility coefficient is a function of the volume and the pressure, $K_T = f(p, V)$. So, the polytropic exponent is $n = f(S, T, V, p)$. Nevertheless, if the dependence of $n$ with the volume is taken into account, it is being assumed that there is a scale effect. So, the volume dependence will not be taken into account. The pressure dependence is cancelled with $K_T$, so finally, $n = f(S, T)$.

The Taylor series of the polytropic exponent around a initial volume $V_0$ can be expressed as:

$$n(V) = n(V_0) + \left.\frac{\partial n}{\partial V}\right|_{V_0} (V - V_0) + \frac{1}{2} \left.\frac{\partial^2 n}{\partial v^2}\right|_{V_0} (V - V_0)^2 + \ldots \tag{26}$$

The polytropic exponent is a function of the entropy and the temperature, so:

$$\frac{\partial n}{\partial V} = \left(\frac{\partial n}{\partial S}\right)_T \left(\frac{\partial S}{\partial V}\right)_T + \left(\frac{\partial n}{\partial T}\right)_S \left(\frac{\partial T}{\partial V}\right)_S \tag{27}$$

On the other hand, $n = f(m, K_T, p)$, so:

$$\left(\frac{\partial n}{\partial S}\right)_T = \left(\frac{\partial n}{\partial m}\right)_T \left(\frac{\partial m}{\partial S}\right)_T + \left(\frac{\partial n}{\partial K_T}\right)_T \left(\frac{\partial K_T}{\partial S}\right)_T + \left(\frac{\partial n}{\partial p}\right)_T \left(\frac{\partial p}{\partial S}\right)_T$$
$$\left(\frac{\partial n}{\partial T}\right)_S = \left(\frac{\partial n}{\partial m}\right)_S \left(\frac{\partial m}{\partial T}\right)_S + \left(\frac{\partial n}{\partial K_T}\right)_S \left(\frac{\partial K_T}{\partial T}\right)_S + \left(\frac{\partial n}{\partial p}\right)_S \left(\frac{\partial p}{\partial T}\right)_S$$

Substituting these expression into (27), the first term of the Taylor expansion is:

$$\frac{\partial n}{\partial V} = \frac{1}{K_T p}\left[\left(\frac{\partial m}{\partial V}\right)_S + \left(\frac{\partial m}{\partial V}\right)_T\right] - \frac{m}{K_T^2 p}\left[\left(\frac{\partial K_T}{\partial V}\right)_S + \left(\frac{\partial K_T}{\partial V}\right)_T\right] - \frac{m}{K_T p^2}\left[\left(\frac{\partial p}{\partial V}\right)_S + \left(\frac{\partial p}{\partial V}\right)_T\right] \tag{28}$$

Naming as $n' = \partial n/\partial V$ in order to simplify, the second term of the Taylor expansion is:

$$\frac{\partial^2 n}{\partial V^2} = \frac{\partial n'}{\partial V} = \left(\frac{\partial n'}{\partial S}\right)_T \left(\frac{\partial S}{\partial V}\right)_T + \left(\frac{\partial n'}{\partial T}\right)_S \left(\frac{\partial T}{\partial V}\right)_S = \left(\frac{\partial n'}{\partial m}\right)\left[\left(\frac{\partial m}{\partial V}\right)_S + \left(\frac{\partial m}{\partial V}\right)_T\right] + \\ + \left(\frac{\partial n'}{\partial K_T}\right)\left[\left(\frac{\partial K_T}{\partial V}\right)_S + \left(\frac{\partial K_T}{\partial V}\right)_T\right] + \left(\frac{\partial n'}{\partial p}\right)\left[\left(\frac{\partial p}{\partial V}\right)_S + \left(\frac{\partial p}{\partial V}\right)_S\right] \tag{29}$$

### *5.1. Ideal gas, adiabatic process*

To get a specific expression of the Taylor expansion from the general expression (26) and from the computed terms (28) and (29), the type of process must be known. In a first approach, let us considerer an adiabatic and reversible process of an ideal gas, which state equation is $pv = R_0 T$, where $v$ is the molar volume. In this case, the entropy is constant, so $C_y = C_s = 0$, $K_T = 1/p$ and $n = m = 1.4$. Applying the state equation to the Taylor expansion, taking into account that the derivarive of $K_T$ with the volume is null and $m$ is constant, the first and second term of this expansion is:

$$\frac{\partial n}{\partial V} = \frac{-m}{K_T p^2}\frac{-2p}{V} = \frac{2m}{K_T p V} = \frac{2n}{V}$$
$$\frac{\partial^2 n}{\partial V^2} = \frac{-2m}{K_T p^2 V}\frac{-2p}{V} = \frac{4m}{K_T p V^2} = \frac{4n}{V^2}$$

Finally, the Taylor expansion of the polytropic exponent for the adiabatic process is cleared out in equation (30):

$$n(V) = n(V_0) + \frac{2n(V_0)}{V_0}(V - V_0) + \frac{2n(V_0)}{V_0^2}(V - V_0)^2 \tag{30}$$

Equation (30) represents a system with reference volume $V_0$ which is essentially governed by a reference polytropic exponent $n(V_0)$. From a thermodynamic point of view,

$n$ should not be expected to change according with its non–dimensional nature. However, the Taylor expansion allows to set a dependence between the polytropic exponent and the system volume variations, which can be used to approach the influence of the system volume scale on the thermodynamic performance. This dependence is represented in Figure 1, where the variation of the polytropic exponent is represented against the air volume in non–dimensional form.

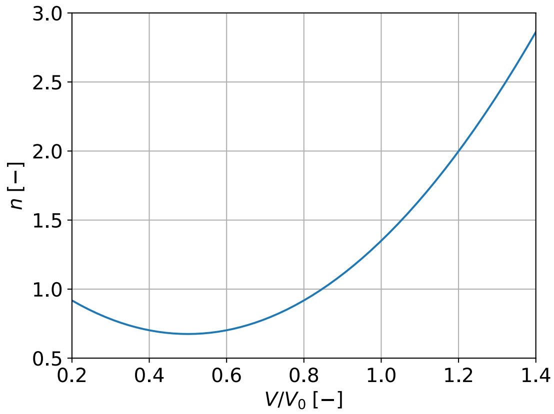


Figure 1: Variation of the polytropic exponent with the non–dimensional volume of the system, according to the instability analysis indicated in eq.(30).

It is clear that according to the rationale, any change with respect to the reference volume $V_0$, i. e. $V/V_0 \neq 1$, is associated with a change in $n$. It can be observed how the system becomes more sensible to the volume variation in terms of the polytropic exponent for larger values of $V/V_0$, say for the greater values of system volume. This different sensibility could be interpreted as a variation in the thermodynamic processes with the variation in scale, affecting the OWC device performance and its efficiency.

It is clear that the nature of the dependence of the polytropic exponent with the system volume variation as represented in equation (30), is fixed by the form of the Taylor expansion. However, on the ground of that dependence, it can be deduced a thermodynamic performance which helps to explain how an increase in volume can affect the nature of the compression/expansion process through the polytropic equation (4) governing it. From a purely qualitative point of view, expression (30) and Figure 1 reveal that as the ratio $V/V_0$ increases, the variation of the polytropic exponent becomes more noticeable. The previous statement is in turn coherent with the fact that non–equilibrium states are intrinsically related with the time–length dimensions involved in the even distribution of state function values over the system volume. Indeed, that conclusion reveals that for an OWC model to be representative of the full–scale thermodynamics, it would require a different enlarged scale for the system volume dimension, so that transient stated in–between equilibrium states to be expected at full–scale, be represented in a more realistic way. This point has been previously suggested by some authors, [65, 12]. In any case, whether the deviation of the polytropic exponent from equilibrium values entirely addresses the theoretical approach in figure 1, or requires further enhancement implementing additional factors, is an open line by the authors of this research.

### *5.2. Case study*

Let us consider a full scale OWC device with a system air volume $V_0$. Following the discussion in §5.1, the variation of the polytropic exponent due to the air volume variations can be estimated. It can be seen from Figure 1 that a shift in this curve can mean either a change in the initial volume $V_0$ due to a change in the escale, or a change in the volume range for a given $V_0$. All in all, any volume oscillation around $V/V_0 \neq 1$ can be interpreted so that the model has a different scale than the prototype.

Now a full–scale device with initial air volume $V_0 = 30\,\mathrm{m}^3$ is compared with a scaled model with air volume $V_{0,m} = V_0/2 = 15\,\mathrm{m}^3$. In both cases, a 20% air volume variation around the initial air volume is applied, which can be a representation of the air volume variation induced by waves. The full–scale device would shift between the values $V/V_0 = [0.8, 1.2]$, and the scaled model between the values $V/V_0 = [0.4, 0.6]$. That means a polytropic exponent variation ranging between $[0.91, 1.99]$ for the full–scale device, and $[0.67, 0.70]$ for scaled model, as figure 2 shows.

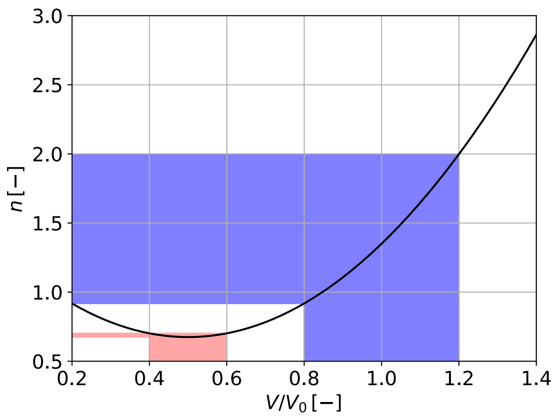


Figure 2: Variation of the polytropic exponent with the non–dimensional volume of the system (according to eq.(30)). The shaded areas indicates the two cases of study. The blue one represent the full–scale device, and the red one the scaled model.

Applying the polytropic process expression in the form $pV^n = \text{const}$, the pressure variation for both cases can be estimated. The pressure values obtained are represented in Figure 3. Figure 3(a) shows the variation of the pressure with the volume, following the polytropic process. It can be observed that the range of pressure variation is different, depending on the scale considered. The pressure variation range is wider for the full scale model than for the reduced scale model, as it was expected due to the range of variation of the polytropic exponent. Nevertheless, according to Froude similarity the relation between the pressures in the prototype and in the model should be linear, see section § 3, but Figure 3(b) shows that this dependence is not linear, which might reveal the existence of scale effects.

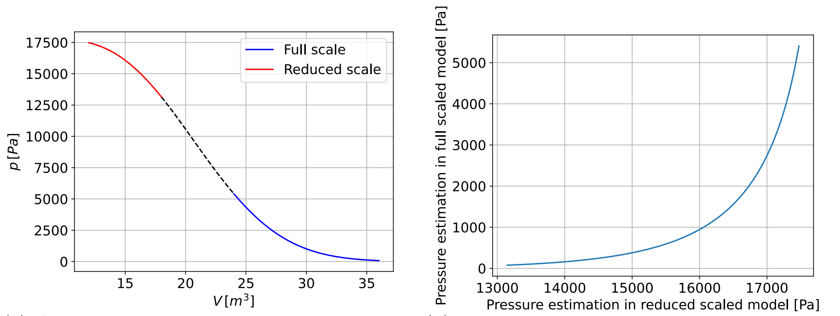


(a) Air pressure variation with the air volume for the two cases studied.

(b) Pressure obtained for the full–scale device vs. pressure obtained for the scaled model.

Figure 3: ressure obtained for the two cases studied.

Those values of pressure can be used to estimate the efficiency of both devices. Let us consider a vertical cylindrical OWC chamber with 2.5 m diameter, which would mean an emergence height of 6.1 m for the prototype and 3.05 m for the scaled model. Now it is considered the implementation of a Wells turbine with performance characteristics similar to Pico plant, [18], with 2.3 m of diameter and a rotational speed of 1500 r.p.m., whose calibration curve and efficiency curve are known. So, with the pressure, volume and polytropic exponent values estimated, the efficiency of the device for the two cases studied can be estimated using the mentioned calibration and efficiency curves. The estimated efficiency is 0.621 for the prototype, and 0.576 for the scaled model. If there were no scale effects, the efficiency in both cases should be the same —since the efficiency is a non–dimensional parameter—, so the differences in the efficiency for both cases can be due to the existence of scale effects, as it has been stated before. In fact, this result agrees with the proposal of [65] and [12] regarding the requirement for an increase in the scaled device volume of the air chamber. In any case, further research is required to implement thermodynamic effects whose scale dependence and extent is not trivial.

In the case of a very small scale, such as the experimental test that can be performed in the laboratory, the results can be different, as all the evidence indicates. Following the same reasoning as before, if the initial volume were 3 m$^3$ ($V_{0,s} = V_0/10$), the efficiency of the device would be $\eta_s = 0.707$. The values estimated in the previous paragraph indicate that $\eta_p > \eta_m$, so one would expect that the smaller the scale, the lower the efficiency obtained. However, the efficiency of the very small device is higher than that of the model and prototype. Thus, scale effects may play an important role at very small scales. In addition, it is important to note that non-equilibrium states become more relevant as the scale increases. Thus, in the very small scale, these non-equilibrium states would not be as obvious.

Similar results are obtained considering an adiabatic process for a real gas, whose state equation is $pv = ZR_0T$. To check the results for a real gas and a non–adiabatic process, the state equation must be known, as well as the variable $y$ that remains constant, in order to obtain a specific expression of the Taylor series.

## 6. Discussion, conclusions and future research

In this research, a theoretical approach to a comprehensive understanding the scale effects in OWC devices has been made. The main advantages and disadvantages of this similarity analysis are:

- Regarding the dynamic and thermodynamic of the OWC, the linearized expansion–compression process allows scaling to compensate for the constraint that the atmospheric pressure be the same in the model and in the prototype.
- Meanwhile, the non–linear model does not allow this correction, which necessarily brings scaling effects that are all the more relevant the more non–linearity is involved and the smaller geometric scale.
- The similarity analysis brings to front the problems that appears when trying to couple the hydrodynamics, thermodynamics and aerodynamics process that occurs in the OWC scaled devices.
- In practical applications, it is difficult to construct a turbine that respects all the scale relations, like the aerodynamic and inertial forces, the inertia of the rotor, the mass of the blades, or the torque, among others.
- According to Froude similarity, the Reynolds number is smaller in the model than in prototype, which influences strongly the structure of the turbulences. This is quite relevant while considering the transport process (heat, momentum, etc.) and affecting strongly the thermodynamics process.
- The Mach number in the scaled model is smaller than in the prototype, according to Froude similarity. That means that the pressure waves have a more damped effect in the model than in the prototype.
- The scaling of the Weber number, which is not unitary following the Froude similarity, affects the thermodynamics of the gas inside the OWC chamber since the gas lacks the characteristics spray and therefore has different properties than in the prototype.
- The research brings to front the fact that, in the case of thermodynamic processes, the phenomena accuracy increases downward scaling from prototype to model, as oposite to other area of similitude analysis, in which accuracy increases upward

scaling from model to prototype. In that sense, the fine tuning of the air chamber scale, regardless the scale adjustment of the rest of variables involved on the problem, helps to increase the accuracy in the real full–scale phenomena from prototype to model.

Whether the scale effect is relevant when approaching a complete wave-to-wire is yet to be analyzed in depth. Not so much from a pure theoretical or numerical way as from an experimental set-up. In any case, this theoretical approach is intended to settle a reference frame for future research on the topic. In addition, the results are consistent with previous experimental/theoretical studies, leading to a better understanding of the point that in the case of the thermodynamics process involved in air compression–expansion inside the chamber, scaled devices provide with a better framework for thermodynamic process to match equilibrium conditions, otherwise mandatory for the application of First and Second Principles of thermodynamics is obviously a counter effect to other processes involved in OWC performance, specially those related with the wave impingement, radiation–diffraction and turbulence, in which large–scale devices provide with more realistic representation of the phenomena. Even if experimental and numerical research are a feasible way to observe all of the above, a theoretical basis is required to set the guidelines.

This research intends to set the basis for the next numerical simulations and experimental test. That new research is meant to focus on the study of the chamber and turbine size, where different configurations will be compared with the aim to check the scale effects. The main conclusions of this research are:

- In the PTO similarity, the linearized process allows scaling to compensate for the constraint that the atmospheric pressure be the same in the model and in the prototype. The full non–linear model does not allow this correction and necessarily brings scaling effects that are all the more relevant the more non–linearity is involved.
- The similarity conditions for the water side implies that the pressure scale in the chamber is linked permanently to the velocity scale in the water column.
- As for the similarity for the turbine, it is difficult to construct a turbine that respect simultaneously all the factors that affect its performance, like the inertia of the rotor, the mass of the propeller, or the friction effects, among others.
- The turbulence plays an important role that must be taken into account, and varies during the two exhalation/inhalation phases. While it is difficult to quantify the scale effects on turbulence, these effects affect to the thermodynamics process.
- A comprehensive approach through instability analysis reveals that the scale size introduces differences in the thermodynamic process at different scales, through the variation of the polytropic exponent values. This fact would imply different efficiency values for the device at different scales. As a first approach, the results reveal that non–equilibrium states, which would be less evident in scaled model according to the sensibility of the polytropic exponent, would become more relevant as the scale is increased towards the size of the prototype.

The contribution of this research to the existing literature is to provide a better understanding of the initial scale effects studies, Weber [65], Falcão & Henriques [12], in the sense that reveals how the thermodynamic scaling requires a different adjustment as the standard scaling applied to other process involved in OWC performance. In fact, the accuracy of thermodynamic processes experimentally simulated increases downward —from full scale to model—, due to the minimization of transient states between equilibrium states, while the rest of process involved in OWC performance gain in accuracy upward —from model to full scale—.

When balancing the scaling on both water side and air side involved in the OWC dimensional problem, there might be a counter–effect in several processes involved. Wave action, turbulence and hydrodynamic pressure is expected to be conditioned and somewhat limited at small scales when compared with full—scale performance. On the contrary, thermodynamic processes directly related with pneumatic performance and efficiency through polytropic process, might be disturbed at larger scales due to transient states required to reach an even distribution of thermodynamic variables over the entire system. This fact could indicate that devices smaller than full–scale plants built nowadays could have a better performance.

The implementation of a numerical model to study scale effects is a matter of study with several difficulties in experience of the Authors of the proposal, Moñino *et al.* [47], Medina-Lopez *et al.* [40]. Even if many aspects can be successfully represented, namely the real gas performance, two-phase air and water model, wave impingement and radiation-diffraction through deformable mesh feature, etc., one of the main issues is the correct representation of the turbine. The free rotation of the turbine driven solely by the air phase displaced by the water phase inside the chamber is difficult to simulate. In fact, the common procedure is to impose a rotation to the turbine domain, which in turn affects the radiation-diffraction and pressure-air flow coupling, or to replace the turbine by an orifice or actuator disk model, Teixeira *et al.* [60], Moñino *et al.* [47]. In both cases, while the pressure peaks in compression and expansion can be successfully represented, all details regarding pressure-volume states through the polytropic process are not properly simulated. For that reason, to retrieve some additional information on scale effects seems to be less reliable that the information deduced from a comprehensive theoretical basis -even if some simplifications are assumed- to be later observed in an experimental model.

In order to continue with this research, the next step would be to conduct some numerical simulations where all the effects indicated above would be analysed. Taking step further, it would be required an experimental study to reproduce the performance of a real–scaled OWC model in a laboratory and to check the results of this research and the numerical simulations. Conceptually, it seems relevant to identify a measure of the distance, in phase space, from the equilibrium condition of the transformations, in order to estimate its value in both the model and the prototype.

## Author contribution

**Ángel Molina**: Analysis, writing & editing.

**Sandro Longo**: Analysis, concept, writing & editing.

**María Clavero**: Project leading, manuscript revision.

**Antonio Moñino**: Project leading, concept, writing & editing.

## Acknowledgement

This work was funded by Andalusian Regional Government, projects P18-RT-3595 and B-RNM-346-UGR18, and Grant TED2021.131717B.I00–GORGONA funded by MCIN/AEI/10.13039/501100011033 and, as appropriate, by the European Union NextGenerationEU/PRTR.

[1] Bingham, Harry B., Ducasse, Damien, Nielsen, Kim & Read, Robert 2015 Hydrodynamic analysis of oscillating water column wave energy devices. *Journal of Ocean Engineering and Marine Energy* **1**, 405–419.

[2] Carballo, R., Sánchez, M., Ramos, V., Fraguela, J. A. & Iglesias, G. 2015 The intra-annual variability in the performance of wave energy converters: A comparative study in N Galicia (Spain). *Energy* **82**, 138–146.

[3] Carbon Trust 2005 Oscillating Water Column Wave Energy Converter Evaluation Report. Marine Energy Challenge. *Tech. Rep.*. The Carbon Trust.

[4] Ciappi, L. 2021 Wave-to-wire modelling of oscillating water column wave energy converters and design optimisation for the mediterranean sea. Phd thesis, University of Florence, available at `https://hdl.handle.net/2158/1245178`.

[5] Ciappi, L., Simonetti, I., Bianchini, A., Cappietti, L. & Manfrida, G. 2022 Application of integrated wave-to-wire modelling for the preliminary design of oscillating water column systems for installations in moderate wave climates. *Renewable Energy* **194**, 232–248.

[6] Clavero, M., Chiapponi, L., Longo, S. & Losada, M. A. 2023 Principles and Laboratory Tests on Wind-Wave Generation, Interaction and Breaking Processes. In *Advances on Testing and Experimentation in Civil Engineering* (ed. C. Chastre, J. Neves, D. Ribeiro, M. G. Neves & P. Faria). Springer Tracts in Civil Engineering.

[7] Cruz, J. 2008 *Ocean wave energy: current status and future prespectives*. Springer Science & Business Media.

[8] Dimakopoulos, A. S., Cooker, M. J. & Bruce, T. 2017 The influence of scale on the air flow and pressure in the modelling of Oscillating Water Column Wave Energy Converters. *International Journal of Marine Energy* **19**, 272–291.

[9] Dimotakis, P. E. 2005 Turbulent mixing. *Annual Review of Fluid Mechanics* **37**, 329–356.

[10] Evans, D. V. 1982 Wave-power absorption by systems of oscillating surface pressure distributions. *Journal of Fluid Mechanics* **114**, 481–499.

[11] Evans, D. V. & Porter, R. 1995 Hydrodynamic characteristics of an oscillating water column device. *Applied Ocean Research* **17** (3), 155–164.

[12] Falcão, A. F. de O. & Henriques, J. C. C. 2014 Model-prototype similarity of oscillating-water-column wave energy converters. *International Journal of Marine Energy* **6**, 18–34.

[13] Falcão, A. F. de O. & Henriques, J. C. C. 2019 The spring-like air compressibility effect in oscillating-water-column wave energy converters: Review and analyses. *Renewable and Sustainable Energy Reviews* **12**, 483–498.

[14] Falcão, A. F. de O., Henriques, J. C. C. & Gato, L. M. C. 2017 Rotational speed control and electrical rated power of an oscillating-water-column wave energy converter. *Energy* **120**, 253–261.

[15] Falcão, A. F. de O., Henriques, J. C. C., Gomes, R. P. F. & Portillo, J. C. C. 2022 Theoretically based correction to model test results of OWC wave energy converters to account for air compressibility effect. *Renewable Energy* **198**, 41–50.
[16] Falcão, A. F. de O. & Justino, P. A. P. 1999 OWC wave energy devices with air flow control. *Ocean Engineering* **26** (12), 1275–1295.
[17] Falnes, J. 2007 A review of wave-energy extraction. *Marine Structures* **20** (4), 185–201.
[18] Falçao, A.F.O., Sarmento, J.N.A., Gato, L.M.C. & Brito-Melo, A. 2020 The Pico OWC Wave Power Plant: Its lifetime from conception to closure 1986-2018. *Applied Ocean Research* **98**, 102104.
[19] Fox, B. N., Gomes, R. P. F. & Gato, L. M. C. 2021 Analysis of oscillating-water-column wave energy converter configurations for integration into caisson breakwaters. *Applied Energy* **295**.
[20] Gato, L. M. C. & Falcão, A. F. de O. 1984 On the theory of the Wells turbine. *Journal of Engineering for Gas Turbines and Power* **106** (3), 628–633.
[21] Gato, L. M. C. & Falcão, A. F. de O. 1989 Aerodynamics of the Wells turbine: Control by swinging rotor-blades. *International Journal of Mechanical Sciences* **31** (6), 425–434.
[22] Gato, L. M. C., Henriques, J. C. C. & Carrelhas, A. A. D. 2022 Sea trial results of the biradial and wells turbines at mutriku wave power plant. *Energy Conversion and Management* **268**, 115936.
[23] Gayé, J. B. 2020 *Formalismos y métodos de la termodinámica*. Reverte.
[24] Gomes, R. P. F., Henriques, J. C. C., Gato, L. M. C. & Falcão, A. F. de O. 2014 Hydrodynamic optimization of an axisymmetric floating oscillating water column for wave energy conversion. *Renewable Energy* **44**, 328–339.
[25] Gurnari, L., Filianoti, P. G. F. & Camporeale, S. M. 2022 Fluid dynamics inside a U-shaped oscillating water column (OWC): 1D vs. 2D CFD model. *Renewable Energy* **193**, 687–705.
[26] Henriques, J.C.C., Portillo, J.C.C., Sheng, W., Gato, L.M.C. & Falcão, A.F.O. 2019 Dynamics and control of air turbines in oscillating-water-column wave energy converters: Analyses and case study. *Renewable and Sustainable Energy Reviews* **112**, 571–589.
[27] Heras-Saizarbitoria, I., Zamanillo, I. & Laskurain, I. 2013 Social acceptance of ocean wave energy: A case study of an OWC shoreline plant. *Renewable and Sustainable Energy Reviews* **27**, 515–524.
[28] Hitzeroth, M. & Megerle, A. 2013 Renewable energy projects: Acceptance risks and their management. *Renewable and Sustainable Energy Reviews* **27**, 576–584.
[29] Huertas-Fernández, F., Clavero, M., Reyes-Merlo, M. Á. & Moñino, A. 2021 Combined Oscillating Water Column & hydrogen electrolysis for wave energy extraction and management. A case study: The Port of Motril (Spain). *Journal of Cleaner Production* **324**, 129143.
[30] Kenko, D. & Gambier, A. 2022 Real-time wind turbine simulation for pitch control purposes by using a hardware-in-the-loop approach. In *Proceedings of the 21st International Conference on Modelling and Applied Simulation MAS 2022*.
[31] Kestin, J. 1966 *A course in thermodynamics*. Waltham: Blaisdell.
[32] Kjelstrup, S., Bedeaux, D., Johannessen, E. & Gross, J. 2020 *Non-equilibrium thermodynamics for engineers*. World Scientific.
[33] Liu, Z., Xu, C., Qu, N., Cui, Y. & Kim, K. 2020 Overall performance evaluation of a model-scale OWC wave energy converter. *Renewable Energy* **149**, 1325–1338.
[34] Longo, S. 2022 *Principles and Applications of Dimensional Analysis and Similarity*. Springer.
[35] Lovas, S., Mei, C. C. & Liu, Y. 2010 Oscillating water column at a coastal corner for wave power extraction. *Applied Ocean Research* **32** (3), 267–283.
[36] Luo, Y., Nader, J.-R., Cooper, P. & Zhu, S.-P. 2014 Nonlinear 2D analysis of the efficiency of fixed Oscillating Water Column wave energy converters. *Renewable Energy* **64**, 255–265.
[37] López, I., Carballo, R., Taveira-Pinto, F. & Iglesias, G. 2020 Sensitivity of OWC performance to air compressibility. *Renewable Energy* **145**, 1334–1347.
[38] Martins-Rivas, H. & Mei, C. C. 2009 Wave power extraction from an oscillating water column along a straight coast. *Ocean Engineering* **36** (6), 426–433.
[39] Martins-Rivas, H. & Mei, C. C. 2009 Wave power extraction from an oscillating water column at the tip of a breakwater. *Journal of Fluid Mechanics* **626**, 395–414.
[40] Medina-Lopez, E., Borthwick, A. G. L. & Moñino, A. 2019 Analytical and numerical simulations of an oscillating water column with humidity in the air chamber. *Journal of Cleaner Production* **238**, 117898.
[41] Medina-López, E., Bergillos, R. J., Moñino, A., Clavero, M. & Ortega-Sánchez, M. 2017 Effects of seabed morphology on oscillating water column wave energy converters. *Energy* **135**, 659–673.

[42] Medina-López, E., Moñino, A., Bergillos, R. J., Clavero, M. & Ortega-Sánchez, M. 2019 Oscillating water column performance under the influence of storm development. *Energy* **166**, 765–774.

[43] Medina-López, E., Moñino, A., Borthwick, A. G. L. & Clavero, M. 2017 Thermodynamics of an OWC containing real gas. *Energy* **135**, 709–717.

[44] Medina-López, E., Moñino, A., Clavero, M., del Pino, C. & Losada, M. A. 2016 Note on a real gas model for OWC performance. *Renewable Energy* **85**, 588–597.

[45] Mendonça, A., Dias, J., Didier, E., Fortes, C. J. E. M., Neves, M. G., Reis, M. T., Conde, J. M. P., Poseiro, P. & Teixeira, P. R. F. 2018 An integrated tool for modelling oscillating water column (OWC) wave energy converters (WEC) in vertical breakwaters. *Journal of Hydro-environment Research* **19**, 198–213.

[46] Molina, A., Jiménez-Portaz, M., Clavero, M. & Moñino, A. 2022 The effect of turbine characteristics on the thermodynamics and compression process of a simple OWC device. *Renewable Energy* **190**, 836–847.

[47] Moñino, A., Medina-López, E., Clavero, M. & Benslimane, S. 2017 Numerical simulation of a simple OWC problem for turbine performance. *International Journal of Marine Energy* **20**, 17–32.

[48] Moñino, A., Quirós, C., Mengíbar, F., Medina-Lopez, E. & Clavero, M. 2020 Thermodynamics of the OWC chamber: Experimental turbine performance under stationary flow. *Renewable Energy* **155**, 317–329.

[49] Ocean, SI 2012 Ocean energy: State of the art. *Tech. Rep.*. Strategic Initiative for Ocean Energy (SI Ocean).

[50] Ocean, SI 2012 Ocean energy technology: gaps and barriers. *Tech. Rep.*. Strategic Initiative for Ocean Energy (SI Ocean).

[51] Ocean, SI 2013 Ocean energy: cost of energy and cost reduction opportunities. *Tech. Rep.*. Strategic Initiative for Ocean Energy (SI Ocean).

[52] Peregrine, D. H. 2003 Water-wave impact on walls. *Annual Review of Fluid Mechanics* **35** (1), 23–43.

[53] Prausnitz, J. M., Lichtenthaler, R. N. & Gomes de Azevedo, E. 1998 *Molecular thermodynamics of fluid-phase equilibria*. Pearson Education.

[54] Raghunathan, S. 1995 The Wells air turbine for wave energy conversion. *Progress in Aerospace Sciences* **31** (4), 335–386.

[55] Rezanejad, K., Bhattacharjee, J. & Guedes Soares, C. 2013 Stepped sea bottom effects on the efficiency of nearshore oscillating water column device. *Ocean Engineering* **70**, 25–38.

[56] Rezanejad, K., Bhattacharjee, J. & Guedes Soares, C. 2015 Analytical and numerical study of dual-chamber oscillating water columns on stepped bottom. *Renewable Energy* **75**, 272–282.

[57] Rezanejad, K., Gadelho, J. F. M., Xu, S. & Guedes Soares, C. 2021 Experimental investigation on the hydrodynamic performance of a new type floating oscillating water column device with dual-chambers. *Ocean Engineering* **234**, 109307.

[58] Sarmento, A. J. N. A. & Falcão, A. F. de O. 1985 Wave generation by an oscillating surface-pressure and its application in wave-energy extraction. *Journal of Fluid Mechanics* **150**, 467–485.

[59] Sheng, W., Alcorn, R. & Lewis, A. 2013 On thermodynamics in the primary power conversion of oscillating water column wave energy converters. *Journal of Renewable and Sustainable Energy* **5**, 023105.

[60] Teixeira, P. R. F., Davyt, D. P., Didier, E. & Ramalhais, R. 2013 Numerical simulation of an oscillating water column device using a code based on Navier–Stokes equations. *Energy* **61**, 513–530.

[61] Tennekes, H. & Lumley, J. L. 1972 *A first course in turbulence*. MIT press.

[62] Thibeaut, F., Griffiths, J., Pellat, A., O'Sullivan, D. & Alcorn, R. 2010 Servomotor controlled piston rig for the simulation of an Oscillating Water Column air chamber. In *3rd International Conference on Ocean Energy (ICOE2010)*.

[63] Tsonopoulos, C. & Heidman, J. L. 1990 From the virial to the cubic equation of state. *Fluid Phase Equilibria* **57** (3), 261–276.

[64] Uihlein, A. & Magagna, D. 2016 Wave and tidal current energy – A review of the current state of research beyond technology. *Renewable and Sustainable Energy Reviews* **58**, 1070–1081.

[65] Weber, J. 2007 Representation of non-linear aero-thermodynamic effects during small scale physical modelling of Oscillating Water Column wave energy converters. In *Proc. 7th European Wave Tidal Energy Conference, Porto, Portugal*.

[66] Wisniak, J. 2003 Heike kamerlingh — the virial equation of state. *IJCT Vol.10(5) [September 2003]* .

[67] World Energy, Council 2016 World energy resources 2016. *World Energy Council* p. 1028.
[68] Zhang, Y., Zou, Q.-P. & Greaves, D. 2012 Air–water two-phase flow modelling of hydrodynamic performance of an oscillating water column device. *Renewable Energy* **41**, 159–170.

## List of Figures

## List of Symbols

$A_c$: Cross–section area of the air chamber – [m$^2$]
$A_{pto}$: Cross–section area of the PTO device – [m$^2$]
$C_r$: Coefficient of resistance – [−−]
$C_y$: Specific heat under constant variable $y$ – [J/(mol K)]
$F_{aer}$: Aerodynamic forces – [N]
$F_{in}$: Inertial forces – [N]
$g$: Gravity aceleration – [m/s$^2$]
$h_0$: Chamber height at rest – [m]
$K_1$: Turbine damping coefficient– [kg/(m$^2$s)]
$K_T$: Isothermal compressibility coefficient – [Pa$^{-1}$]
$Ma$: Mach number – [−−]
$m$: Mass of air – [kg]
$m$: Polytropic index – [−−]
$n$: Polytropic exponent – [−−]
$p$: Pressure – [Pa]
$p_{0c}$: Pressure inside the chamber when $\eta = 0$ – [Pa]
$p_a$: Atmospheric pressure – [Pa]
$p_c$: Air chamber pressure – [Pa]
$r_{(\ldots)}$: Ratio between the value of the variable $(\ldots)$– [−−]
$\tilde{p}_c$: Relative pressure in the chamber – [Pa]
$Q_m$: Mass flow – [kg/m$^3$]
$R_0$: Universal gas constant – [8.31 J/(K mol)]
$Re$: Reynolds number – [−−]
$S$: Entropy – [J/K]
$T$: Temperature – [K]
$t$: Time – [s]
$V$: Air volume – [m$^3$]
$V_0$: Initial air volume of the chamber – [m$^3$]
$v$: Space average air velocity – [m/s]
$v$: Molar volume – [m$^3$/mol]
$We$: Weber number – [−−]
$\ddot{x}$: Acceleration – [m/s$^2$]
$z$: Vertical direction – [m]

Greek
$\gamma$: Polytropic exponent for adiabatic process – [−−]
$\eta$: Instantaneous cross–average water level in the chamber – [m]
$\lambda$: Length scale factor – [−−]
$\nu$: Kinematic viscosity – [m$^2$/s]
$\rho_a$: Air density – [kg/m$^3$]
$\rho_c$: Gas density inside the chamber – [kg/m$^3$]
$\rho_w$: Water density – [kg/m$^3$]
$\Phi$: Potential function – [m$^2$/s]